EUROPEAN LABORATORY FOR PARTICLE PHYSICS (CERN)

CERN PPE/97-129
September 23, 1997

Search for charged Higgs bosons in e^+e^- collisions at centre-of-mass energies from 130 to 172 GeV

The ALEPH Collaboration*)

Abstract

The data collected at centre-of-mass energies ranging from 130 to 172 GeV by ALEPH at LEP, corresponding to an integrated luminosity of 27.5 pb^{-1}, are analysed in a search for pair-produced charged Higgs bosons $H^{\pm}$. Three analyses are employed to select the $\tau^+\nu_\tau\tau^-\bar{\nu}_\tau$, $c\bar{s}\tau^-\bar{\nu}_\tau$ and $c\bar{s}s\bar{c}$ final states. No evidence for a signal is found. Mass limits are set as a function of the branching fraction $\mathcal{B}(\tau\nu)$ for $H^{\pm} \to \tau\nu$. Charged Higgs bosons with masses below 52 GeV/c^2 are excluded at 95% C.L. independently of $\mathcal{B}(\tau\nu)$, thus significantly improving on existing limits.

(Submitted to Physics Letters B)

---

*) See next pages for the list of authors

The ALEPH Collaboration

R. Barate, D. Buskulic, D. Decamp, P. Ghez, C. Goy, J.-P. Lees, A. Lucotte, M.-N. Minard, J.-Y. Nief, B. Pietrzyk

Laboratoire de Physique des Particules (LAPP), IN^{2}P^3-CNRS, 74019 Annecy-le-Vieux Cedex, France

M.P. Casado, M. Chmeissani, P. Comas, J.M. Crespo, M. Delfino, E. Fernandez, M. Fernandez-Bosman, Ll. Garrido,[15] A. Juste, M. Martinez, G. Merino, R. Miquel, Ll.M. Mir, C. Padilla, I.C. Park, A. Pascual, J.A. Perlas, I. Riu, F. Sanchez

Institut de Física d'Altes Energies, Universitat Autònoma de Barcelona, 08193 Bellaterra (Barcelona), Spain[7]

A. Colaleo, D. Creanza, M. de Palma, G. Gelao, G. Iaselli, G. Maggi, M. Maggi, N. Marinelli, S. Nuzzo, A. Ranieri, G. Raso, F. Ruggieri, G. Selvaggi, L. Silvestris, P. Tempesta, A. Tricomi,[3] G. Zito

Dipartimento di Fisica, INFN Sezione di Bari, 70126 Bari, Italy

X. Huang, J. Lin, Q. Ouyang, T. Wang, Y. Xie, R. Xu, S. Xue, J. Zhang, L. Zhang, W. Zhao

Institute of High-Energy Physics, Academia Sinica, Beijing, The People's Republic of China[8]

D. Abbaneo, R. Alemany, A.O. Bazarko,[1] U. Becker, P. Bright-Thomas, M. Cattaneo, F. Cerutti, G. Dissertori, H. Drevermann, R.W. Forty, M. Frank, F. Gianotti, R. Hagelberg, J.B. Hansen, J. Harvey, P. Janot, B. Jost, E. Kneringer, I. Lehraus, P. Mato, A. Minten, L. Moneta, A. Pacheco, J.-F. Pusztaszeri,[20] F. Ranjard, G. Rizzo, L. Rolandi, D. Rousseau, D. Schlatter, M. Schmitt, O. Schneider, W. Tejessy, F. Teubert, I.R. Tomalin, H. Wachsmuth, A. Wagner[21]

European Laboratory for Particle Physics (CERN), 1211 Geneva 23, Switzerland

Z. Ajaltouni, A. Barrès, C. Boyer, A. Falvard, C. Ferdi, P. Gay, C . Guicheney, P. Henrard, J. Jousset, B. Michel, S. Monteil, J-C. Montret, D. Pallin, P. Perret, F. Podlyski, J. Proriol, P. Rosnet, J.-M. Rossignol

Laboratoire de Physique Corpusculaire, Université Blaise Pascal, IN^{2}P^3-CNRS, Clermont-Ferrand, 63177 Aubière, France

T. Fearnley, J.D. Hansen, J.R. Hansen, P.H. Hansen, B.S. Nilsson, B. Rensch, A. Wäänänen

Niels Bohr Institute, 2100 Copenhagen, Denmark[9]

G. Daskalakis, A. Kyriakis, C. Markou, E. Simopoulou, A. Vayaki

Nuclear Research Center Demokritos (NRCD), Athens, Greece

A. Blondel, J.C. Brient, F. Machefert, A. Rougé, M. Rumpf, A. Valassi,[6] H. Videau

Laboratoire de Physique Nucléaire et des Hautes Energies, Ecole Polytechnique, IN^{2}P^3-CNRS, 91128 Palaiseau Cedex, France

T. Boccali, E. Focardi, G. Parrini, K. Zachariadou

Dipartimento di Fisica, Università di Firenze, INFN Sezione di Firenze, 50125 Firenze, Italy

R. Cavanaugh, M. Corden, C. Georgiopoulos, T. Huehn, D.E. Jaffe

Supercomputer Computations Research Institute, Florida State University, Tallahassee, FL 32306-4052, USA [13,14]

A. Antonelli, G. Bencivenni, G. Bologna,[4] F. Bossi, P. Campana, G. Capon, D. Casper, V. Chiarella, G. Felici, P. Laurelli, G. Mannocchi,[5] F. Murtas, G.P. Murtas, L. Passalacqua, M. Pepe-Altarelli

Laboratori Nazionali dell'INFN (LNF-INFN), 00044 Frascati, Italy

L. Curtis, S.J. Dorris, A.W. Halley, I.G. Knowles, J.G. Lynch, V. O'Shea, C. Raine, J.M. Scarr, K. Smith, P. Teixeira-Dias, A.S. Thompson, E. Thomson, F. Thomson, R.M. Turnbull

Department of Physics and Astronomy, University of Glasgow, Glasgow G12 8QQ,United Kingdom[10]

O. Buchmüller, S. Dhamotharan, C. Geweniger, G. Graefe, P. Hanke, G. Hansper, V. Hepp, E.E. Kluge, A. Putzer, J. Sommer, K. Tittel, S. Werner, M. Wunsch

Institut für Hochenergiephysik, Universität Heidelberg, 69120 Heidelberg, Fed. Rep. of Germany[16]

R. Beuselinck, D.M. Binnie, W. Cameron, P.J. Dornan, M. Girone, S. Goodsir, E.B. Martin, P. Morawitz, A. Moutoussi, J. Nash, J.K. Sedgbeer, P. Spagnolo, A.M. Stacey, M.D. Williams

Department of Physics, Imperial College, London SW7 2BZ, United Kingdom[10]

V.M. Ghete, P. Girtler, D. Kuhn, G. Rudolph

Institut für Experimentalphysik, Universität Innsbruck, 6020 Innsbruck, Austria[18]

A.P. Betteridge, C.K. Bowdery, P.G. Buck, P. Colrain, G. Crawford, A.J. Finch, F. Foster, G. Hughes, R.W.L. Jones, T. Sloan, E.P. Whelan, M.I. Williams

Department of Physics, University of Lancaster, Lancaster LA1 4YB, United Kingdom[10]

I. Giehl, C. Hoffmann, K. Jakobs, K. Kleinknecht, G. Quast, B. Renk, E. Rohne, H.-G. Sander, P. van Gemmeren, C. Zeitnitz

Institut für Physik, Universität Mainz, 55099 Mainz, Fed. Rep. of Germany[16]

J.J. Aubert, C. Benchouk, A. Bonissent, G. Bujosa, J. Carr, P. Coyle, C. Diaconu, A. Ealet, D. Fouchez, N. Konstantinidis, O. Leroy, F. Motsch, P. Payre, M. Talby, A. Sadouki, M. Thulasidas, A. Tilquin, K. Trabelsi

Centre de Physique des Particules, Faculté des Sciences de Luminy, IN^{2}P^3-CNRS, 13288 Marseille, France

M. Aleppo, M. Antonelli, F. Ragusa

Dipartimento di Fisica, Università di Milano e INFN Sezione di Milano, 20133 Milano, Italy.

R. Berlich, W. Blum, V. Büscher, H. Dietl, G. Ganis, C. Gotzhein, H. Kroha, G. Lütjens, G. Lutz, W. Männer, H.-G. Moser, R. Richter, A. Rosado-Schlosser, S. Schael, R. Settles, H. Seywerd, R. St. Denis, H. Stenzel, W. Wiedenmann, G. Wolf

Max-Planck-Institut für Physik, Werner-Heisenberg-Institut, 80805 München, Fed. Rep. of Germany[16]

J. Boucrot, O. Callot,[12] S. Chen, M. Davier, L. Duflot, J.-F. Grivaz, Ph. Heusse, A. Höcker, A. Jacholkowska, D.W. Kim,[2] F. Le Diberder, J. Lefrançois, A.-M. Lutz, M. Marumi, M.-H. Schune, L. Serin, E. Tournefier, J.-J. Veillet, I. Videau, D. Zerwas

Laboratoire de l'Accélérateur Linéaire, Université de Paris-Sud, IN^{2}P^3-CNRS, 91405 Orsay Cedex, France

P. Azzurri, G. Bagliesi,[12] S. Bettarini, C. Bozzi, G. Calderini, V. Ciulli, R. Dell'Orso, R. Fantechi, I. Ferrante, A. Giassi, A. Gregorio, F. Ligabue, A. Lusiani, P.S. Marrocchesi, A. Messineo, F. Palla, G. Sanguinetti, A. Sciabà, G. Sguazzoni, J. Steinberger, R. Tenchini, C. Vannini, A. Venturi, P.G. Verdini

Dipartimento di Fisica dell'Università, INFN Sezione di Pisa, e Scuola Normale Superiore, 56010 Pisa, Italy

G.A. Blair, L.M. Bryant, J.T. Chambers, M.G. Green, T. Medcalf, P. Perrodo, J.A. Strong, J.H. von Wimmersperg-Toeller

Department of Physics, Royal Holloway & Bedford New College, University of London, Surrey TW20 OEX, United Kingdom[10]

D.R. Botterill, R.W. Clifft, T.R. Edgecock, S. Haywood, P. Maley, P.R. Norton, J.C. Thompson, A.E. Wright

Particle Physics Dept., Rutherford Appleton Laboratory, Chilton, Didcot, Oxon OX11 OQX, United Kingdom[10]

B. Bloch-Devaux, P. Colas, B. Fabbro, E. Lançon, M.C. Lemaire, E. Locci, P. Perez, J. Rander, J.-F. Renardy, A. Rosowsky, A. Roussarie, J. Schwindling, A. Trabelsi, B. Vallage

CEA, DAPNIA/Service de Physique des Particules, CE-Saclay, 91191 Gif-sur-Yvette Cedex, France[17]

S.N. Black, J.H. Dann, H.Y. Kim, A.M. Litke, M.A. McNeil, G. Taylor

Institute for Particle Physics, University of California at Santa Cruz, Santa Cruz, CA 95064, USA[19]

C.N. Booth, C.A.J. Brew, S. Cartwright, F. Combley, M.S. Kelly, M. Lehto, J. Reeve, L.F. Thompson

Department of Physics, University of Sheffield, Sheffield S3 7RH, United Kingdom[10]

K. Affholderbach, A. Böhrer, S. Brandt, G. Cowan, J. Foss, C. Grupen, L. Smolik, F. Stephan

Fachbereich Physik, Universität Siegen, 57068 Siegen, Fed. Rep. of Germany[16]

M. Apollonio, L. Bosisio, R. Della Marina, G. Giannini, B. Gobbo, G. Musolino

Dipartimento di Fisica, Università di Trieste e INFN Sezione di Trieste, 34127 Trieste, Italy

J. Putz, J. Rothberg, S. Wasserbaech, R.W. Williams

Experimental Elementary Particle Physics, University of Washington, WA 98195 Seattle, U.S.A.

S.R. Armstrong, E. Charles, P. Elmer, D.P.S. Ferguson, Y. Gao, S. González, T.C. Greening, O.J. Hayes, H. Hu, S. Jin, P.A. McNamara III, J.M. Nachtman, J. Nielsen, W. Orejudos, Y.B. Pan, Y. Saadi, I.J. Scott, J. Walsh, Sau Lan Wu, X. Wu, J.M. Yamartino, G. Zobernig

Department of Physics, University of Wisconsin, Madison, WI 53706, USA[11]

---

[1]Now at Princeton University, Princeton, NJ 08544, U.S.A.

[2]Permanent address: Kangnung National University, Kangnung, Korea.

[3]Also at Dipartimento di Fisica, INFN Sezione di Catania, Catania, Italy.

[4]Also Istituto di Fisica Generale, Università di Torino, Torino, Italy.

[5]Also Istituto di Cosmo-Geofisica del C.N.R., Torino, Italy.

[6]Supported by the Commission of the European Communities, contract ERBCHBICT941234.

[7]Supported by CICYT, Spain.

[8]Supported by the National Science Foundation of China.

[9]Supported by the Danish Natural Science Research Council.

[10]Supported by the UK Particle Physics and Astronomy Research Council.

[11]Supported by the US Department of Energy, grant DE-FG0295-ER40896.

[12]Also at CERN, 1211 Geneva 23,Switzerland.

[13]Supported by the US Department of Energy, contract DE-FG05-92ER40742.

[14]Supported by the US Department of Energy, contract DE-FC05-85ER250000.

[15]Permanent address: Universitat de Barcelona, 08208 Barcelona, Spain.

[16]Supported by the Bundesministerium für Bildung, Wissenschaft, Forschung und Technologie, Fed. Rep. of Germany.

[17]Supported by the Direction des Sciences de la Matière, C.E.A.

[18]Supported by Fonds zur Förderung der wissenschaftlichen Forschung, Austria.

[19]Supported by the US Department of Energy, grant DE-FG03-92ER40689.

[20]Now at School of Operations Research and Industrial Engireering, Cornell University, Ithaca, NY 14853-3801, U.S.A.

[21]Now at Schweizerischer Bankverein, Basel, Switzerland.

1 Introduction

In the minimal Standard Model of electroweak interactions, the Higgs sector comprises only one doublet of complex scalar fields. As a result, the theory contains only one additional physical state, electrically neutral, the so-called standard Higgs boson. Despite the success of the Standard Model, no direct experimental information is available on the Higgs sector. The investigation of the implications of more complicated Higgs sectors, both in the context of the Standard Model and in extended theories, is therefore necessary.

The most important phenomenological consequence of an extended Higgs structure is the appearance of additional physical scalar states. For example, in the simplest extensions of the minimal Standard Model (the two-doublet models), one additional doublet of complex scalar fields is introduced. Five scalar physical states remain after the spontaneous symmetry breaking mechanism has given mass to $\mathrm{W}^{\pm}$ and Z gauge bosons: three neutral bosons and a pair of charged scalar bosons. Among the possible choices, multi-doublet models are theoretically interesting because they naturally lead, at tree level, to $m_{\mathrm{W}} = m_{\mathrm{Z}} \cos\theta_{\mathrm{W}}$ ($m_{\mathrm{W}}, m_{\mathrm{Z}}$ and θ_{W} being, respectively, the W and Z masses and the electroweak mixing angle) and to the absence of flavour changing neutral currents, two major constraints that must be satisfied by any extension of the Standard Model to agree with the experimental observations. Another reason of interest in such models comes from the fact that one version of the two-doublet model represents the minimal Higgs sector for "low-energy" supersymmetric theories [1].

This letter describes a search for pair production of the charged Higgs bosons $\mathrm{H}^{\pm}$ predicted in two-Higgs-doublet extensions of the Standard Model. The analysis uses the data collected by the ALEPH detector in $\mathrm{e}^{+}\mathrm{e}^{-}$ collisions delivered by LEP at centre-of-mass energies of 130 (2.8 pb^{-1}), 136 (2.9 pb^{-1}), 161 (11.1 pb^{-1}), 170 (1.1 pb^{-1}) and 172 GeV (9.6 pb^{-1}).

Pair production of charged Higgs bosons occurs mainly via s-channel exchange of a photon or a Z boson; in two-doublet models, the couplings are completely specified in terms of the electric charge and θ_{W}, making the production cross section depend only on one additional parameter, the charged Higgs boson mass m_{H}. The basic decay channel of the charged Higgs boson is $\mathrm{H}^{+} \to \mathrm{f_u}\bar{\mathrm{f}}_{\mathrm{d}}$, where $\mathrm{f_u}$ ($\mathrm{f_d}$) is an up-type (down-type) fermion. The possibility of additional decay channels depends on the details of the models. For example, in minimal supersymmetry several decays involving supersymmetric partners can occur. However, because the sensitivity of this analysis is limited to Higgs boson masses well below the W mass, and given the present negative results of searches for supersymmetric particles, the contribution of the additional channels to the $\mathrm{H}^{\pm}$ decay width is not expected to be significant. It is therefore assumed that the $\mathrm{H}^{\pm}$ decays mostly into matter fermions. Furthermore the decay lifetime is assumed to be negligible. This is justified by the fact that in the two-doublet implementations studied so far [1], vanishing decay widths either are not possible or require a rather unnatural choice of the parameters (ratio of Higgs vacuum expectation values either very small or very large). Although the choice of Higgs-fermion

couplings is not unique [1], there is a common feature determining the phenomenology of the reaction, namely the proportionality of the coupling to fermion masses and to the relevant CKM matrix element [1]. As a consequence the predominant decays are expected to be $H^+ \to c\bar{s}$ or $H^+ \to \tau^+\nu_\tau$ (and the respective charge conjugates for H^-). Since the relative weight of these two main channels depends on the details of the model, no assumption is made about the decay branching fractions, and three different selections are developed to address the possible final states $c\bar{s}s\bar{c}$, $c\bar{s}\tau^-\bar{\nu}_\tau$ and $\tau^+\nu_\tau\tau^-\bar{\nu}_\tau$. Under the same hypothesis, the negative results of the searches performed using the first 8.5 pb^{-1} of data collected at LEP 1 allowed ALEPH to exclude charged Higgs masses less than 41.7 GeV/c^2 at 95% C.L., independently of the final state [2]. Excluded domains up to 44.1 GeV/c^2 were also reported by the L3 and OPAL collaborations [3]. DELPHI excludes charged Higgs bosons up to 47 GeV/c^2 in mass, using the data recorded at centre-of-mass energies up to 161 GeV [4]. Less general limits have also been set by ALEPH [5], CLEO [6] and CDF [7].

The letter is organised as follows. After the description of the relevant parts of the ALEPH detector in Section 2, the Monte Carlo samples used for the analysis are described in Section 3. The event selections are detailed in Section 4. The results and the conclusions are given in Sections 5 and 6.

2 The ALEPH Detector

The ALEPH detector is described in detail in Ref. [8]. An account of the performance of the detector and a description of the standard analysis algorithms can be found in Ref. [9]. Here, only a brief description of the detector components and the algorithms relevant for this analysis is given.

In ALEPH, the trajectories of charged particles are measured with a silicon vertex detector, a cylindrical drift chamber, and a large time projection chamber (TPC). These are immersed in a 1.5 T axial field provided by a superconducting solenoidal coil. The electromagnetic calorimeter, placed between the TPC and the coil, is a highly segmented sampling calorimeter which is used to identify electrons and photons and to measure their energy. The luminosity monitors extend the calorimetric coverage down to 24 mrad from the beam axis. An additional shielding against beam related background installed before the 1996 running reduces the acceptance by 10 mrad. The hadron calorimeter consists of the iron return yoke of the magnet instrumented with streamer tubes. It provides a measurement of hadronic energy and, together with the external muon chambers, muon identification.

The calorimetry and tracking information are combined in an energy flow algorithm, classifying a set of energy flow "particles" as photons, neutral hadrons and charged particles. Hereafter, charged particle tracks reconstructed with at least four hits in the TPC, and originating from within a cylinder of length 20 cm and radius 2 cm coaxial with the beam and centred at the nominal collision point, will be referred to as *good tracks*.

3 Monte Carlo Samples

Fully simulated Monte Carlo event samples reconstructed with the same program as the data have been used for background estimates, design of selections and cut optimisation. Samples of all major background sources corresponding to at least 20 times the collected luminosity were generated. The most important background sources are $e^+e^- \to \tau^+\tau^-$, $q\bar{q}$ and four-fermion processes (including WW production), simulated with `KORALZ` [10] and `PYTHIA` [11].

The signal Monte Carlo events for selection design and efficiency calculation were generated using a version of `HZHA` [12] extended for charged Higgs boson production. The initial state radiation is implemented, both for event generation and cross section calculation, by means of the `REMT` package [13], modified to account for the $\alpha^2_{\rm QED}$ part of the spectrum. In the case of the hadronic decay, the hadronisation of the $c\bar{s}$ system is performed with `JETSET` [11]; if both H^+ and H^- decay hadronically, the resulting diquark systems are hadronised independently. In the case of $H^+ \to \tau^+\nu_\tau$, the τ polarisation is transmitted to the `TAUOLA` library [14], called for the subsequent τ decay.

Samples of at least 1000 signal events were simulated for each of the various final states for charged Higgs boson masses between 40 and 70 GeV/c^2, and for each centre-of-mass energy.

4 Event selections

To ensure a good discovery potential independent of the branching fraction $\mathcal{B}(\tau\nu)$ for the decay of the Higgs boson into $\tau\nu$, three selections are defined for the topologies $\tau^+\nu_\tau\tau^-\bar{\nu}_\tau$, $c\bar{s}\tau^-\bar{\nu}_\tau$ and $c\bar{s}s\bar{c}$. The most relevant selection criteria for the three selections are chosen in order to achieve, on average and in case no signal is present, the best 95% C.L. limit on the Higgs boson production cross section [15]. Each individual selection is optimised independently, taking the most optimistic $\mathcal{B}(\tau\nu)$ in each case, *i.e.*, 0% for the $c\bar{s}s\bar{c}$ channel, 50% for the $c\bar{s}\tau^-\bar{\nu}_\tau$ channel, and 100% for the $\tau^+\nu_\tau\tau^-\bar{\nu}_\tau$ channel. In the following sections, the three sets of selection criteria are described in detail. The performance of the analyses is summarised in Table 1 and Table 2, showing efficiencies for different Higgs boson masses and the expected background from Standard Model processes.

4.1 The $\tau^+\nu_\tau\tau^-\bar{\nu}_\tau$ final state

The final state produced by leptonic decays of the two charged Higgs bosons consists of two acoplanar τ's and missing energy carried away by the neutrinos. Since this topology is very similar to that defined in connection with the search for staus, the selections described in [16] and [17] are used here to search for charged Higgs bosons in the $\tau^+\nu_\tau\tau^-\bar{\nu}_\tau$ channel at $\sqrt{s}$ = 130–136 GeV and 161–172 GeV, respectively. These selections exploit the fact

final state	$\tau^+\nu_\tau\tau^-\bar{\nu}_\tau$			$c\bar{s}\tau^-\bar{\nu}_\tau$			$c\bar{s}s\bar{c}$		
$\sqrt{s}$ (GeV)	133	161	172	133	161	172	133	161	172
$\epsilon(45\ \mathrm{GeV}/c^2)$	46	42	38	72	54	51	25	35	35
$\epsilon(50\ \mathrm{GeV}/c^2)$	51	45	40	71	54	50	26	38	37
$\epsilon(55\ \mathrm{GeV}/c^2)$	55	48	41	64	51	47	25	36	38
$\epsilon(60\ \mathrm{GeV}/c^2)$	58	49	43	44	42	35	22	35	38

Table 1: Efficiencies (in %) for the three analyses at the three centre-of-mass energies, given for four different Higgs masses between 45 GeV/c^2 and 60 GeV/c^2. Efficiencies in the four jet channel are quoted within a ± 3 GeV/c^2 window around the generated Higgs boson mass.

selection	expected background			candidate events
	130, 136 GeV	161 GeV	172 GeV	130–172 GeV
$\tau^+\nu_\tau\tau^-\bar{\nu}_\tau$	1.0	0.5	1.0	1
$c\bar{s}\tau^-\bar{\nu}_\tau$	0.3	0.8	1.0	0
$c\bar{s}s\bar{c}$	3.1	7.9	7.7	14

Table 2: Expected number of background events from Standard Model processes for Higgs masses less than 70 GeV/c^2, in comparison with the number of events observed in the data.

that the signal events contain at least four neutrinos, leading to large missing energy and a large acoplanarity of the visible system. Background from WW production followed by leptonic W decays is suppressed by vetoing events with energetic electrons or muons, which are expected to be softer when originating from τ decays.

Efficiencies to select events from $H^+H^- \to \tau^+\nu_\tau\tau^-\bar{\nu}_\tau$ are of the order of 45% at $\sqrt{s} = 161$–172 GeV, as shown in Table 1 for a representative set of Higgs boson masses. The total background expected amounts to 1.0 event at $\sqrt{s} = 130$–136 GeV and 1.5 events at $\sqrt{s} = 161$–172 GeV (Table 2), the latter mainly consisting of irreducible background from $W^+W^- \to \tau^+\nu_\tau\tau^-\bar{\nu}_\tau$. In the data, one event is selected at $\sqrt{s} = 161$ GeV.

4.2 The $c\bar{s}\tau^-\bar{\nu}_\tau$ final state

The mixed final state ($c\bar{s}\tau^-\bar{\nu}_\tau$ or $\bar{c}s\tau^+\nu_\tau$) is characterised by two jets originating from the hadronic decay of one of the charged Higgs and a thin τ jet plus missing energy due to the neutrinos from the decay of the other Higgs boson.

The analysis is based on two complementary approaches. In one selection, called the *global* analysis, global quantities such as acoplanarity, thrust, and missing momentum are predominantly used whereas the second selection, referred to as the *topological* analysis, relies more on the specific τ jet reconstruction. The analyses were designed for a centre-

of-mass energy of 161 GeV. However, only minor modifications are necessary for the data recorded at 172 GeV and 130–136 GeV, which will be mentioned explicitly in the description of the analyses. Events are accepted if they pass the topological or the global analysis. For the data recorded at 130 GeV and 136 GeV, where the WW background is not present, the global analysis is replaced by the more efficient inclusive combination of two analyses published in [16]. These selections, designed for the chargino searches for large mass differences, are applied here raising the cut on the visible mass $M_{\rm vis}$ to 40 GeV/c^2 and excluding the analyses with purely leptonic final states.

A preselection is common to both analyses: at least seven good tracks with polar angles greater than 18.2° are required. The energy measured within a cone of half-angle 12° around the beam axis must be less than $2.5\%\sqrt{s}$ in order to reduce the background from tagged $\gamma\gamma$ interactions and $\mathrm{q\bar{q}}$ events with an initial state radiation photon detected at low angle. The visible mass of the event must be greater than 40 GeV/c^2 and less than 140 GeV/c^2 (172 GeV: 150 GeV/c^2, 130–136 GeV: 120 GeV/c^2). The quadratic mean of the inverse of the hemisphere boosts, introduced in [16], is required to be greater than 0.3. At least three jets must be reconstructed with the JADE algorithm using a $y_{\rm cut}$ of 0.001.

In the global analysis, to reject $\mathrm{q\bar{q}}$ events where an initial state radiation photon escapes undetected in the beam pipe, the acoplanarity angle between the two hemisphere momentum directions is required to be less than 175°. The event thrust must be less than 0.9, and the missing transverse momentum is required to amount to at least 20% of the visible energy. The missing transverse momentum direction is expected to be isolated in the signal, but not in the $\mathrm{q\bar{q}}$ background. The energy contained in an azimuthal wedge of half angle 30° with respect to the missing transverse momentum direction is therefore required to be less than $7.5\%\sqrt{s}$.

In order to reject WW events in which one W decays directly to an electron or muon and a neutrino, the momentum of the leading identified lepton is required to be less than $15\%\sqrt{s}$. To deal with events in which the identified lepton originates from a cascade decay via a τ, it is required that the hadronic mass of the event, *i.e.*, the visible mass excluding the leading lepton, be less than 80 GeV/c^2. To cope with the WW background when the τ decays hadronically, jets with at least one and at most three tracks are considered as τ jet candidates. Ambiguities are resolved by first demanding that the total momentum carried by the charged particles of the τ jet candidates be greater than $2.5\%\sqrt{s}$ and then, if necessary, taking the jet closest to being antiparallel to the missing momentum as the τ jet. This is the typical W configuration at 161 GeV where the W's are produced at rest. The other jets are merged to form the two quark jets. Since the sensitivity of this analysis is limited to charged Higgs boson masses well below the W mass, the invariant mass of the quark jets is required to be less than 70 GeV/c^2. Similarly, the acollinearity angle between the two jets is smaller for a Higgs boson decay than for a W decay. This acollinearity is therefore required to be less than 130° (172 GeV: 100°).

In the topological analysis global quantities are also used, but the cuts are loosened with respect to the global analysis. The energy in the 30° wedge with respect to the

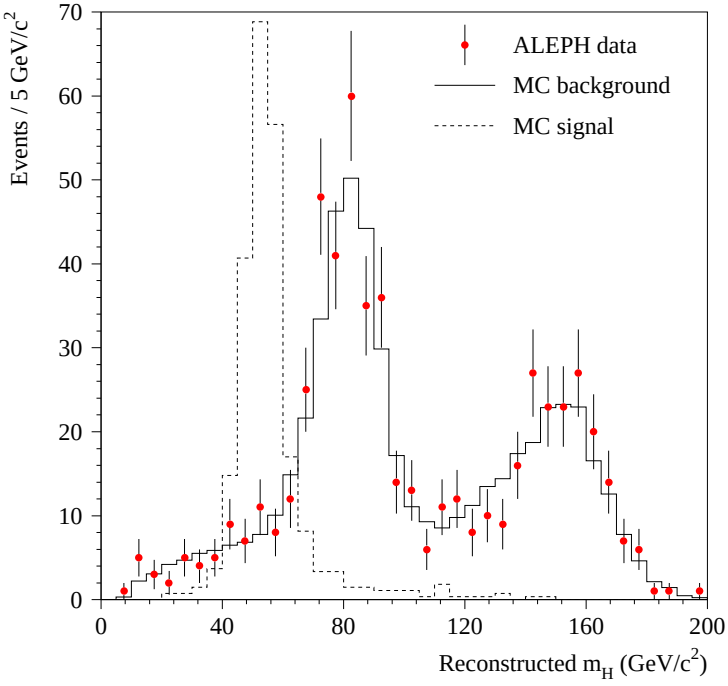

Figure 1: Distribution of the invariant mass of the quark jets, as used in the $c\bar{s}\tau^-\bar{\nu}_\tau$ selection in the topological analysis. The dots are the data collected at $\sqrt{s} = 161$ GeV and 172 GeV, while the full line is the background expectation, normalised to the recorded luminosity. The dashed line is the distribution for a signal with a Higgs boson mass of 55 GeV/c^2 at 161 GeV, arbitrarily normalised. Only a subset of the cuts is applied here to preserve sufficient statistics.

missing transverse momentum direction is required to be less than $20\%\sqrt{s}$, the momentum of the leading lepton must be less than $20\%\sqrt{s}$, the hadronic mass is required to be less than 80 GeV/c^2 (the last cut is not applied at 130–136 GeV), and the missing momentum direction must point more than 25.8° away from the beam axis.

Jets with only one charged particle track are considered as τ jet candidates and their momentum must be greater than $2.5\%\sqrt{s}$. The remaining ambiguities are resolved by choosing the jet whose angle with the missing momentum is closest to 80° as the τ jet (this angle being optimal for Higgs masses in the range 50 to 60 GeV/c^2). Events are rejected either if the angle between the τ jet and any other jet direction is less than 25° or if the invariant mass formed by the other jets (Fig. 1) is greater than 60 GeV/c^2. Finally, the acollinearity angle (defined as above in the global analysis) is required to be less than 140° (172 GeV: 120°, 130–136 GeV: 150°).

Typical efficiencies and the background for this analysis are given in Tables 1 and 2. The main contributions to the systematic error (3%) are the Monte Carlo statistics, the

luminosity measurement (<1%) and the requirement of the maximum energy observed within 12° of the beam pipe (<2%), which was studied using events triggered at random beam crossings. No events are selected in the data while in total 2.1 events are expected from the Standard Model background.

4.3 The $c\bar{s}s\bar{c}$ final state

For this channel, the hadronic decays of the two charged Higgs bosons lead to a final state of four well separated jets, which can be combined into two dijets with equal mass. Before exploiting the mass information, a preselection is applied to identify four-jet final states.

Since the cross sections for the two dominant background processes ($e^+e^- \to q\bar{q}$ and $e^+e^- \to W^+W^- \to q\bar{q}q\bar{q}$) depend strongly on the centre-of-mass energy, some of the cuts described in the following vary with $\sqrt{s}$. Spherical events with at least eight good tracks, a minimum charged energy of $10\%\sqrt{s}$ and thrust less than 0.9 (0.8 at $\sqrt{s} = 130$–136 GeV) are clustered into four jets using the Durham algorithm. To select events with four well separated jets, a minimum Durham distance y_{34} of 0.006 (0.008) is required between all the jets. Events from $q\bar{q}(\gamma)$ with an energetic initial state radiation photon undetected at small polar angles are suppressed by requiring the missing momentum p_z^{miss} along the beam axis to be less than $1.5 \times (M_{\mathrm{vis}} - 90)$ ($0.75 \times (M_{\mathrm{vis}} - 90)$ at $\sqrt{s} = 130$–136 GeV). Background with initial state radiation photons in the detector is rejected by removing events with jets that have more than 90% of their energy classified as electromagnetic energy.

At this stage charged Higgs bosons are selected with an efficiency of about 75%. A total background of 153 events is expected, mainly consisting of events from $e^+e^- \to q\bar{q}$ and $W^+W^- \to q\bar{q}q\bar{q}$. The background from $q\bar{q}$ events is suppressed further by requiring the jets to be consistent with originating in the decay of two particles with equal mass. As a first step, four-momentum conservation is imposed on the event to rescale the energies of the four jets, fixing the jet velocities at their measured values. After combining the jets into two dijet systems, a mass difference Δm between the two dijets is calculated for all three possible combinations. Events are selected if the minimum Δm is less than 10 GeV/c^2.

Secondly, for the remaining events, the jet momenta are determined by means of a five-constraint fit, imposing energy-momentum conservation and an equal mass for the dijet systems. This method leads to a dijet mass resolution of about 1.2 GeV/c^2 for a 50 GeV/c^2 Higgs at $\sqrt{s} = 161$ GeV. Events consistent with the equal mass hypothesis are selected by requiring that the χ^2 (Fig. 2) be less than 4.3 (tightened to 2.3 at 130–136 GeV as determined by the optimisation procedure described in [15]) for the dijet combination with the best fit.

Since, given the amount of data collected so far, the sensitivity is limited to masses well below m_{W}, most of the background from WW is not relevant for this analysis. However, in a non-negligible fraction of the WW events, a wrong jet combination gives the best fit, leading to combinatorial background at small masses. For $\sqrt{s} = 172$ GeV, this background is suppressed by vetoing events with a fitted mass m_2 (as obtained from the second best

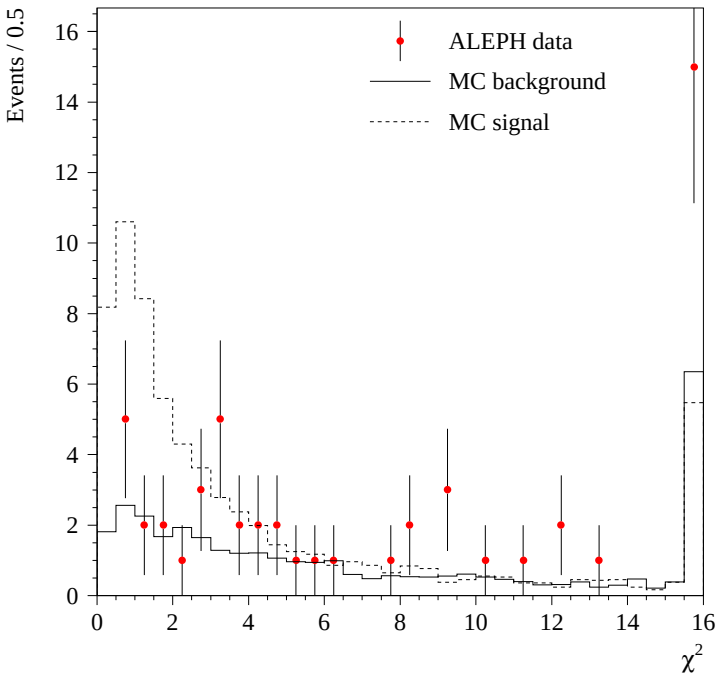

Figure 2: The χ^2 for the dijet combination giving the best fit, plotted for reconstructed masses less than 60 GeV/c^2 after applying the four-jet preselection. The points represent the data at $\sqrt{s} = 130$–172 GeV. The dashed line shows the signal distribution (with arbitrary normalisation) for a Higgs boson mass of 50 GeV/c^2. Overflows are summed in the last bin.

fit) close to the W mass ($|m_2 - m_{\mathrm{W}}| < 2$ GeV/c^2), but only if the dijet mass difference Δm_2 is less than 7 GeV/c^2. Furthermore, background from both $\mathrm{q\bar{q}}$ and WW is reduced by exploiting differences in the distributions of the decay angle θ_{dec} and the production angle θ_{prod}, by means of a single cut $\cos\theta_{\mathrm{prod}} + 0.5\cos\theta_{\mathrm{dec}} < 1$. Here, the decay angle is defined as the angle between the dijet momentum (the "Higgs boson" momentum) and the direction of the two jets in the Higgs boson rest frame, whereas the angle between the beam axis and the Higgs boson momentum is referred to as the production angle.

After these cuts, the total background expected for reconstructed charged Higgs boson masses lower than 70 GeV/c^2 amounts to 18.7 events, summed over all centre-of-mass energies (Table 2). Efficiencies are of the order of 35% within a dijet mass window of ± 3 GeV/c^2 around the Higgs boson mass (Table 1). Because of the relatively higher background level from $\mathrm{q\bar{q}}$, the selection cuts at $\sqrt{s} = 130$–136 GeV are tighter than at higher energy, leading to a lower efficiency at this energy.

The excess of four-jet events previously observed is not consistent with the equal mass hypothesis [18]. Most of these events show up as an excess at large values of χ^2 (Fig. 2)

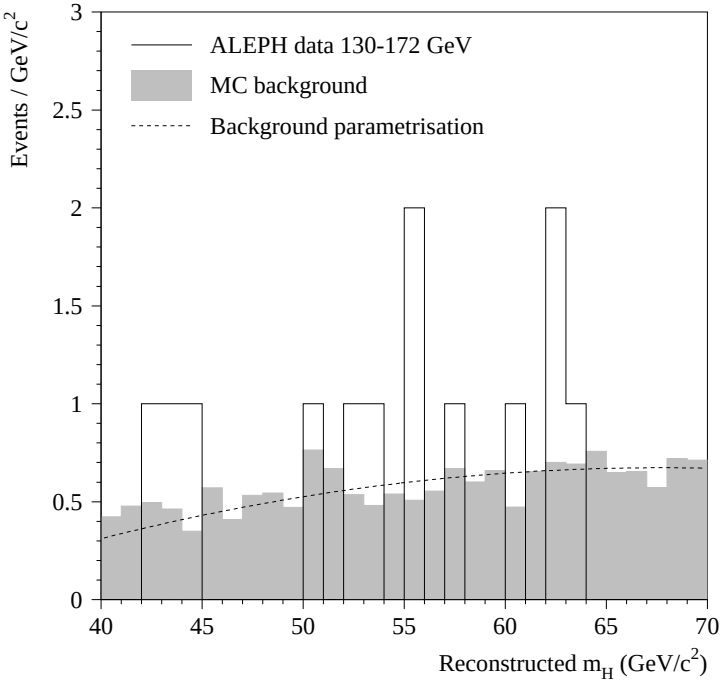

Figure 3: Distribution of the dijet mass as obtained from the five-constraint fit, applying all cuts of the $c\bar{s}s\bar{c}$ selection.

and are therefore not selected by this analysis.

Given the level of irreducible background, the sensitivity of the analysis is considerably increased by subtracting the expected background from Standard Model processes as described in the following section. For this purpose the dijet mass distribution as obtained from the background Monte Carlo is parametrised by a polynomial. The comparison with the data (Fig. 3) shows that the parametrisation is compatible with the observation. In the following, this background estimate is conservatively reduced by 20%, corresponding to the statistical uncertainty of this comparison.

The systematic error on the efficiency is estimated to be 2%, dominated by the Monte Carlo statistical uncertainty, with small additional contributions from the luminosity measurement and energy flow reconstruction [19].

5 Results

In the data collected at centre-of-mass energies from 130 to 172 GeV, a total of 15 events are retained by the three selections presented in Section 4 (one event in the $\tau^+\nu_\tau\tau^-\bar{\nu}_\tau$ channel, fourteen events in the $c\bar{s}s\bar{c}$ channel, and none in the mixed channel) for reconstructed

charged Higgs boson masses less than 70 GeV/c^2, consistent with the 23.3 events expected from Standard Model processes (Table 2). Since, in addition, the mass distribution in the $c\bar{s}s\bar{c}$ channel does not show any significant accumulation (Fig. 3), the result of the three selections are combined to set a 95% C.L. limit on the charged Higgs boson mass, as described in the following paragraphs. In all cases systematic errors are taken into account by conservatively reducing the selection efficiency by one standard deviation.

First, the confidence level is determined for each of the three selections as explained in Ref. [20], as a function of m_{H} and $\mathcal{B}(\tau\nu)$. In the $\tau^+\nu_\tau\tau^-\bar{\nu}_\tau$ and $c\bar{s}\tau^-\bar{\nu}_\tau$ channels, where no background subtraction is performed, the confidence level is conservatively defined as the fraction of outcomes of all possible experiments *with signal only* of mass m_{H} and branching fraction $\mathcal{B}(\tau\nu)$ for which the number of events selected would be smaller than or equal to the number of events observed in the data. No mass information is included in this procedure.

For the $c\bar{s}s\bar{c}$ channel, where background subtraction is performed, the confidence level is defined as the fraction of outcomes of all possible experiments *with signal and background* of mass m_{H} and branching fraction $\mathcal{B}(\tau\nu)$, for which the number of events selected in a mass window of ± 3 GeV/c^2 around m_{H} would be smaller than or equal to the number of events observed in this window. In order not to benefit from the fact that fewer events than expected from Standard Model processes might be observed in that window, this confidence level is renormalised to the fraction of outcomes of all possible experiments *with background only* that satisfy the same condition. This procedure was verified to always lead to a conservative estimate of the confidence level for a given signal hypothesis.

The three confidence levels thus obtained are then combined, for all values of m_{H} and $\mathcal{B}(\tau\nu)$, according to the democratic prescription of Ref. [20], by computing the fraction of all possible experiment outcomes that would lead to a value of the product of the three individual confidence levels smaller than or equal to the observed product.

The result of the combination is displayed in Fig. 4, where the curves corresponding to confidence levels of 0.1%, 1%, 5% (equivalent to a 95% C.L. exclusion), 10% and 30% are drawn. Also shown are the domains excluded at 95% C.L. by the three individual analyses. Charged Higgs bosons with masses less than 52 GeV/c^2 are excluded at 95% confidence level independently of $\mathcal{B}(\tau\nu)$.

6 Conclusions

A search for pair-produced charged Higgs bosons in the three final states $\tau^+\nu_\tau\tau^-\bar{\nu}_\tau$, $c\bar{s}\tau^-\bar{\nu}_\tau$ and $c\bar{s}s\bar{c}$ has been performed using 27.5 pb^{-1} of data collected at $\sqrt{s} = 130$–172 GeV. No evidence of Higgs boson production was found and mass limits were set as a function of $\mathcal{B}(\tau\nu)$. Charged Higgs bosons with masses below 52 GeV/c^2 are excluded at 95% C.L. independently of $\mathcal{B}(\tau\nu)$, improving on the existing limits.

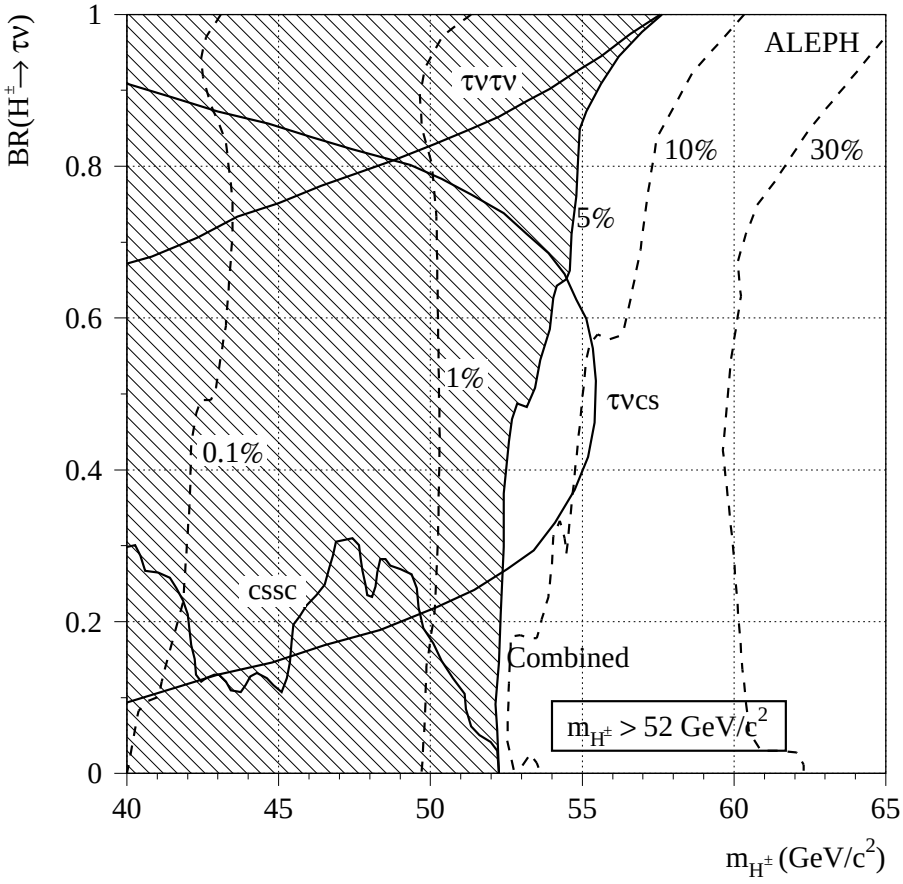

Figure 4: Limit at 95% C.L. on the mass of charged Higgs bosons as a function of $\mathcal{B}(\tau\nu)$. The three solid curves show the 95% C.L. domains excluded by each of the three single analyses, whereas the hatched region is excluded by the combination of all three channels. The dashed curves indicate various combined confidence level values.

7 Acknowledgements

It is a pleasure to congratulate our colleagues from the accelerator divisions for the successful operation of LEP above the W threshold. We are indebted to the engineers and technicians in all our institutions for their contribution to the excellent performance of ALEPH. Those of us from non-member states wish to thank CERN for its hospitality and support.

References

[1] J. F. Gunion, H. E. Haber, G. Kane and S. Dawson, *"The Higgs Hunter's Guide"*, Frontiers in Physics, Lecture Note Series, Addison Wesley, 1990.

[2] ALEPH Collaboration, Phys. Rep. **216** (1992) 253.

[3] L3 Collaboration, Z. Phys. **C 57** (1993) 355;
OPAL Collaboration, Phys. Lett. **B 370** (1996) 174.

[4] DELPHI Collaboration, *"Search for Neutral and Charged Higgs Bosons in e^+e^- Collisions at $\sqrt{s}$ = 161 GeV and 172 GeV"*, CERN-PPE/97-085 (1997), submitted to Z. Phys. C.

[5] ALEPH Collaboration, Phys. Lett. **B 343** (1995) 444.

[6] CLEO Collaboration, Phys. Rev. Lett. **74** (1995) 2885.

[7] CDF Collaboration, *"Search for Charged Higgs Decays of the Top Quark using Hadronic Decays of the Tau Lepton"*, FERMILAB-PUB-97/058-E (1997), submitted to Phys. Rev. Lett.

[8] ALEPH Collaboration, Nucl. Instr. Meth. **A 294** (1990) 121.

[9] ALEPH Collaboration, Nucl. Instr. Meth. **A 360** (1995) 481.

[10] S. Jadach and Z. Wąs, Comp. Phys. Comm. **36** (1985) 191.

[11] T. Sjöstrand, *"The PYTHIA 5.7 and JETSET 7.4 Manual"*, LU-TP 95/20, CERN-TH 7112/93, Comp. Phys. Comm. **82** (1994) 74.

[12] P. Janot, *"The HZHA Generator"* in *"Physics at LEP2"*, Eds. G. Altarelli, T. Sjöstrand and F. Zwirner, CERN 96-01 (1996), Vol. 2, 309.

[13] F. A. Berends and R. Kleiss, *"Radiative Effects in Higgs Production at LEP"*, Nucl. Phys. **178** (1981) 141.

[14] R. Decker, S. Jadach and Z. Wąs, Comp. Phys. Comm. **76** (1993) 361.

[15] J.-F. Grivaz and F. Le Diberder, *"Complementary Analyses and Acceptance Optimization in new Particle Searches"*, LAL preprint # 92-37 (1992).

[16] ALEPH Collaboration, Phys. Lett. **B 373** (1996) 246.

[17] ALEPH Collaboration, *"Search for Sleptons in e^+e^- Collisions at centre-of-mass Energies of 161 GeV and 172 GeV"*, CERN-PPE/97-056 (1997), to be published in Phys. Lett. B.

[18] ALEPH Collaboration, Z. Phys. **C 71** (1996) 179.

[19] ALEPH Collaboration, *"Search for the Neutral Higgs Bosons of the MSSM in e^+e^- Collisions at $\sqrt{s}$ from 130 to 172 GeV"*, CERN-PPE/97-071 (1997), to be published in Phys. Lett. B.

[20] P. Janot and F. Le Diberder, *"Combining Limits"*, CERN-PPE/97-053 (1997), to be published in Nucl. Instr. Meth.